

ULASJ1234 + 0907: The Reddest Type 1 Quasar at $z = 2.5$ Revealed in the X-ray and Far Infra-red ^{*}

Manda Banerji^{1†}, A. C. Fabian² & R. G. McMahon^{2,3}

¹*Department of Physics & Astronomy, University College London, Gower Street, London WC1E 6BT, UK.*

²*Institute of Astronomy, University of Cambridge, Madingley Road, Cambridge, CB3 0HA, UK.*

³*Kavli Institute for Cosmology, University of Cambridge, Madingley Road, Cambridge, CB3 0HA, UK.*

20 August 2019

ABSTRACT

We present *Herschel* and *XMM-Newton* observations of ULASJ1234+0907 ($z = 2.503$), the reddest broad-line Type 1 quasar currently known with $(i - K)_{AB} > 7.1$. *Herschel* observations indicate that the quasar host is a hyperluminous infrared galaxy (HyLIRG) with a total infrared luminosity of $\log_{10}(L_{\text{IR}}/L_{\odot}) = 13.90 \pm 0.02$. A greybody fit gives a dust temperature of $T_d = 60 \pm 3 \text{ K}$ assuming an emissivity index of $\beta = 1.5$, considerably higher than in submillimeter bright galaxies observed at similar redshifts. The star formation rate is estimated to be $> 2000 M_{\odot} \text{ yr}^{-1}$ even accounting for a significant contribution from an AGN component to the total infrared luminosity or requiring that only the far infra-red luminosity is powered by a starburst. *XMM-Newton* observations constrain the hard X-ray luminosity to be $L_{2-10 \text{ keV}} = 1.3 \times 10^{45} \text{ erg/s}$ putting ULASJ1234+0907 among the brightest X-ray quasars known. Through very deep optical and near infra-red imaging of the field at sub-arcsecond seeing, we demonstrate that despite its extreme luminosity, it is highly unlikely that ULASJ1234+0907 is being lensed. We measure a neutral hydrogen column density of $N_H = 9.0 \times 10^{21} \text{ cm}^{-2}$ corresponding to $A_V \sim 6$. The observed properties of ULASJ1234+0907 - high luminosity and Eddington ratio, broad lines, moderate column densities and significant infra-red emission from re-processed dust - are similar to those predicted by galaxy formation simulations for the AGN *blowout* phase. The high Eddington ratio combined with the presence of significant amounts of dust, is expected to drive strong outflows due to the effects of radiation pressure on dust. We conclude that ULASJ1234+0907 is a prototype galaxy caught at the peak epoch of galaxy formation, which is transitioning from a starburst to optical quasar via a dusty quasar phase.

Key words: galaxies:active, (galaxies:) quasars: emission lines, (galaxies:) quasars: general, (galaxies:) quasars: individual

1 INTRODUCTION

Since the discovery of the correlation between the mass of the galactic bulge in galaxies and the mass of their central black holes (Magorrian et al. 1998), understanding the link between the formation and evolution of massive galaxies and their supermassive black holes (SMBH; 10^5 - $10^{10} M_{\text{sun}}$) has become one of the most important problems in both galaxy formation and extreme astrophysics. The realisation that an active SMBH or active galactic nucleus (AGN) plays a fundamental role in determining the final stel-

lar mass of the galactic bulge has wide implications, and has led to the ubiquitous adoption of AGN *feedback* in many galaxy formation models (Croton et al. 2006). Without AGN feedback, these galaxy formation models cannot reproduce the observed number counts of the most massive galaxies.

In cosmological simulations the most massive galaxies in the Universe are assembled at high redshift through gas-rich mergers of smaller systems (Hopkins et al. 2008). The merger is expected to induce a far infrared (FIR) luminous starburst, which enshrouds the galaxy in dust therefore obscuring it completely at ultraviolet (UV) and optical wavelengths. The high gas densities in the merging starburst feed accretion onto the central black hole, which is initially also dust obscured. As radiative pressure on the dust grains begins to clear the dust and gas away during the *blowout* phase (Di Matteo et al. 2005), the central active galactic nucleus (AGN)

^{*} *Herschel* is an ESA space observatory with science instruments provided by European-led Principal Investigator consortia and with important participation from NASA.

[†] E-mail: m.banerji@ucl.ac.uk

is revealed as a UV-luminous quasar. Several indirect lines of evidence suggest that powerful starbursts and luminous quasars occur in the same galaxies (Coppin et al. 2008; Hickox et al. 2012). However, direct observational evidence for starburst galaxies at high redshifts transitioning to UV-luminous quasars, has remained elusive.

In Banerji et al. (2012, 2013) - B12,B13 hereafter - we used infrared surveys to identify 14 extremely massive, luminous, dusty broad-line quasars at $z \sim 2$ that could represent galaxies caught during the AGN blowout phase. This new population of quasars is too dusty to be present in optical surveys like the Sloan Digital Sky Survey (SDSS) that have so far been used to identify the most luminous quasars in the Universe. The reddest and most intrinsically luminous quasar in our current sample is ULASJ1234+0907 at $z = 2.503$. Our spectroscopic observations in B12 detected very broad $H\alpha$ emission from this quasar signifying the presence of an extremely massive SMBH ($\sim 3 \times 10^{10} M_{\odot}$) and/or significant outflows that could be broadening the $H\alpha$ line. This broad emission line also supports the interpretation that the dust responsible for the red colours of the quasar, originates on large scales within the quasar host, rather than in a molecular torus. In the latter case, our view of the quasar broad-line region would have also been blocked for most lines of sight. The dust extinction implied by our SED fit to the broadband colours of ULASJ1234+0907, is $A_V = 6$ mags even accounting for the effect of the large $H\alpha$ equivalent width on the ($H - K$) colour (see B12 for details).

If ULASJ1234+0907 is being observed in the AGN blowout phase, the next step is to look for evidence for a massive starburst quasar host. In this paper, we present detailed multi-wavelength observations of this quasar. X-ray observations with *XMM-Newton* allow us to directly detect the primary accreting power source while far infrared and submillimeter observations with *Herschel* and SCUBA-2 are used to place the first constraints on the quasar host galaxy. Throughout this paper we assume a flat Λ CDM cosmology. All magnitudes are on the AB system with conversion from the Vega system using zeropoint offsets for UKIDSS and *WISE* photometry from Hewett et al. (2006) and Cutri et al. (2012)

2 OBSERVATIONS

2.1 Optical and Near Infra-red Imaging

We conducted i -band imaging of the quasar using the Wide-Field Camera on the 2.5m ISAAC Newton Telescope in April and May 2008. The total exposure time was 85 minutes. The six individual exposures were reduced, stacked and photometrically calibrated onto the SDSS AB system following González-Solares et al. (2011). ULASJ1234+0907 was undetected in the stacked i -band image (Figure 1) with a 5σ magnitude limit of 25.15 giving an ($i - K$) colour of >7.1 . ULASJ1234+0907 is therefore among the reddest extragalactic sources known. Figure 2 of B12 shows the ($i - K$) colours of various well-known extremely red objects. The reddest quasar from that figure: PKSJ0132 which was the reddest quasar previously known (Gregg et al. 2002) has an ($i - K$)=4.2, almost 3 mags bluer than ULASJ1234+0907.

We conducted K_S band observations of ULASJ1234+0907 using the ISAAC camera on the Very Large Telescope. Data was taken in March 2013 under photometric conditions and in very good seeing of $<0.5''$. The observations were taken using 15 dithered exposures of 60s and reduced using standard ESO tools provided as part of the *gasgano* package. The resulting K -band image shown in Figure 1 goes down to a 10σ depth of 23.2.

Table 1. Summary of Multi-wavelength Observations of ULASJ1234+0907 at $z = 2.503$

Instrument & Band	Flux Density
INT i	$<0.316 \mu\text{Jy} (5\sigma)$
WFCAM Y	$<0.435 \mu\text{Jy} (5\sigma)$
WFCAM J	$4.06 \pm 1.10 \mu\text{Jy}$
WFCAM H	$25.9 \pm 4.9 \mu\text{Jy}$
WFCAM K	$219.4 \pm 6.1 \mu\text{Jy}$
WISE $3.4\mu\text{m}$	$0.48 \pm 0.02 \text{ mJy}$
WISE $4.6\mu\text{m}$	$1.14 \pm 0.04 \text{ mJy}$
WISE $12\mu\text{m}$	$6.27 \pm 0.23 \text{ mJy}$
WISE $22\mu\text{m}$	$10.1 \pm 1.6 \text{ mJy}$
<i>Herschel</i> -PACS $70\mu\text{m}$	$41 \pm 4 \text{ mJy}$
<i>Herschel</i> -PACS $100\mu\text{m}$	$58 \pm 6 \text{ mJy}$
<i>Herschel</i> -PACS $160\mu\text{m}$	$83 \pm 8 \text{ mJy}$
<i>Herschel</i> -SPIRE $250\mu\text{m}$	$57 \pm 9 \text{ mJy}$
<i>Herschel</i> -SPIRE $350\mu\text{m}$	$59 \pm 9 \text{ mJy}$
<i>Herschel</i> -SPIRE $500\mu\text{m}$	$50 \pm 12 \text{ mJy}$
SCUBA-2 $850\mu\text{m}$	$<12 \text{ mJy} (3\sigma)$

2.2 Far Infrared and Submillimeter Photometry: *Herschel* & SCUBA-2

Herschel (Pilbratt et al. 2010) Director's Discretionary Time observations were obtained in December 2012 with PACS (Poglitsch et al. 2010). Data was taken in mini scanmap mode using a scan speed of $20''/\text{s}$ and a scan leg length of $3'$ with exposure times in the range of 444 to 895s at $70\mu\text{m}$, $100\mu\text{m}$ and $160\mu\text{m}$. PACS maps were produced with the default pixel scale of $1.4''$, $1.7''$ and $2.8''$ at 70, 100 and $160\mu\text{m}$ respectively using *Herschel* Level 1 data products and the map-making software *Scanamorphos* (Roussel 2012). Fluxes were measured by performing annular aperture photometry at the quasar position using apertures of $5.5''$, $5.6''$ and $10.5''$ at 70, 100 and $160\mu\text{m}$ respectively. The background was measured using apertures of $[20,25]''$ at 70 and $100\mu\text{m}$ and $[24,28]''$ at $160\mu\text{m}$. Appropriate aperture corrections were applied to these fluxes (Poglitsch et al. 2010). Statistical errors on the fluxes were determined by taking the standard deviation of aperture fluxes calculated in blank fields on the combined maps. Systematic flux calibration errors of 5% were added in quadrature to these. The final fluxes and errors are presented in Table 1 and the PACS cutout at $100\mu\text{m}$ is shown in Figure 1.

Herschel-SPIRE data at 250, 350 and $500\mu\text{m}$, is available as part of the *Herschel* Virgo Cluster Survey (HeViCS; Davies et al. 2010) in the HeViCS V3 field. We used the Level 1 processed data from the *Herschel* Science Archive. Timeline fitting was done on each of the 4 orthogonal scans within HIPE using sourceExtractor-Timeline. In several cases, the timeline fitting produced fluxes for one of the scans that was inconsistent with the remaining scans at the level of 20%. We therefore rejected the most discrepant scan from the set of four observations and took the final SPIRE flux to be the median value of the remaining scans. Colour corrections of 0.912, 0.916 and 0.901 at 250, 350 and $500\mu\text{m}$ were applied, appropriate for a typical dusty source with spectral index $\alpha = 3$. The final fluxes are presented in Table 1. Error estimates from the timeline fitting were very similar from scan to scan: $\sim 8\text{mJy}$, 8mJy and 10mJy at 250, 350 and $500\mu\text{m}$ respectively. Our final errors include the calibration uncertainty assumed to be 7% (Bendo et al. 2013) in addition to the PSF fitting errors.

SCUBA-2 service time observations (s12au01; PI:Banerji) were taken in April 2012. The source was observed in *Daisy* mode for 20 minutes and the data was reduced using the SubMillimeter

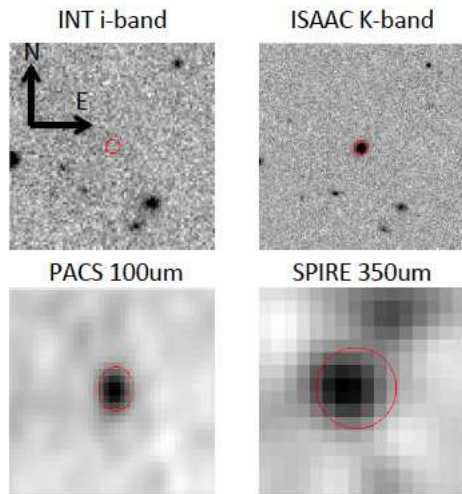


Figure 1. Multi-wavelength images of ULASJ1234+0907 taken with various instruments. The INT *i*-band and ISAAC K_S -band images are $30 \times 30''$ while the *Herschel* cut-outs are $2 \times 2'$ in size. In all cases, the direction of north and east are as specified in the *i*-band image. The quasar position is circled in all images with the size of the circle roughly corresponding to the beam size at that particular wavelength.

User Reduction Facility (SMURF) iterative map maker software to construct an $850\mu\text{m}$ flux density map of the quasar using the default configuration parameters for blank fields. The reduced image has a mean RMS of 4mJy. The quasar was undetected in this $850\mu\text{m}$ image leading to a 3σ upper limit of $S_{850} < 12\text{mJy}$ for ULASJ1234+0907.

2.3 X-ray Observations

X-ray data for ULASJ1234+0907 was obtained using the the European Photon Imaging Camera (EPIC) on the *XMM-Newton* satellite (Jansen et al. 2001). The total exposure time is 42ks for the pn detectors and 52ks for the MOS detectors. Thin filters were used. The total pn source count is 470. A spectrum was extracted in a $21.6''$ aperture around the target. The background was measured from the same chip at a radius of $1.2'$ from the source. The X-ray spectrum from the pn detector can be seen in Figure 3. The MOS detectors are less sensitive but the spectrum obtained from these is consistent with Figure 3.

3 ANALYSIS

3.1 SED Fitting and Star Formation in ULASJ1234+0907

We fit a spectral energy distribution (SED) model to the observed photometry of ULASJ1234+0907 summarised in Table 1. Fitting the SED in the far infrared requires us to disentangle the contribution of the AGN and the starburst to the total infrared luminosity. We adopt two approaches for the SED fitting. Firstly, we use the publicly available SED fitting code CIGALE (Noll et al. 2009), which allows us to fit for both the AGN and starburst components at infrared wavelengths. In this code, the fractional contribution of the AGN to the total infrared luminosity is left as a free parameter in the fitting. The code uses the semi-empirical models of Dale & Helou

(2002) to model the dust emission at infrared wavelengths. AGN templates can additionally be incorporated and we adopt 32 AGN templates from the library of Fritz et al. (2006), encompassing a range of torus opening angles, density parameters, optical depths and outer and inner radii of the dust clouds. We note that the inclusion of other AGN templates available within CIGALE, does not significantly change our results.

Our second approach is simpler with fewer free parameters and allows direct comparison with greybody fits to the SEDs of other high redshift galaxy populations. We use the code developed by Casey (2012) to fit a single temperature greybody and a power-law of the form $S_\lambda \propto \lambda^\alpha$, to model the mid infrared emission at rest-frame wavelengths $\gtrsim 3\mu\text{m}$. The power-law approximates the contribution from an AGN-heated warm dust component.

Using the CIGALE fit we find that the total infrared luminosity is $\log_{10}(L_{\text{TIR}}) = 13.90 \pm 0.02$ with the AGN contribution to this IR luminosity fit to be $62 \pm 4\%$. The starburst luminosity is therefore $\log_{10}(L_{\text{SB}}) = 13.5 \pm 0.1$ which translates to a star formation rate of $\sim 4500 \pm 900 M_\odot \text{yr}^{-1}$ using the Kennicutt & Evans (2012) relation: $\text{SFR} = 3.89 \times 10^{-44} \times L_{\text{SB}} (\text{ergs}^{-1})$. Despite the AGN dominating the infrared dust emission, the SED fitting indicates that this AGN cannot account for all of the infrared emission and the host galaxy of ULASJ1234+0907 must also be forming stars at a prodigious rate. With an inferred starburst luminosity of $> 10^{13} L_\odot$, it can be classified as a hyperluminous infrared galaxy or HyLIRG.

In the case of the single greybody fit, we fix the dust emissivity index to $\beta = 1.5$ (Priddey et al. 2003) due to a lack of photometric data over the Rayleigh-Jeans tail of the SED. The free parameters are the power-law slope, α in the MIR as well as the dust temperature. Although the AGN is expected to dominate the total infra-red luminosity, the far infra-red luminosity between $40\text{--}300\mu\text{m}$ can safely be attributed to a starburst (Rowan-Robinson 2000). We integrate our best-fit single greybody SED between 40 and $300\mu\text{m}$ and use this as a conservative estimate of the total amount of star formation. The infrared luminosity between $40\text{--}300\mu\text{m}$, $L_{40\text{--}300\mu\text{m}} = 1.3 \times 10^{13} L_\odot$ corresponding to a star formation rate of $\sim 2000 \pm 500 M_\odot \text{yr}^{-1}$. The mid infra-red power law slope is relatively shallow: $\alpha = 1.03 \pm 0.03$, which is consistent with the presence of a significant warm dust component from AGN heated dust. The best-fit cold dust temperature is also significantly higher than seen in most submillimeter galaxies: $T_d = 60 \pm 3\text{K}$. The corresponding dust-mass is $\log_{10}(M_{\text{dust}}/M_\odot) = 8.94 \pm 0.08$.

In Figure 2, we also show the SED of the archetypal starburst/AGN composite galaxy Mrk231 in the local Universe which has been scaled to have the same flux density as ULASJ1234+0907 at a rest-frame wavelength of $6\mu\text{m}$. Finally we plot the composite far infrared SED of the high luminosity ($\log(L_{2\text{--}10\text{keV}}) > 42.9$) X-ray AGN from Mullaney et al. (2011) again scaled to ULASJ1234+0907 at a rest-frame wavelength of $6\mu\text{m}$. ULASJ1234+0907 has a higher mid to far infra-red flux ratio than Mrk231. The pure AGN SED on the other hand, drops rapidly at rest-frame wavelengths of $\gtrsim 40\mu\text{m}$ whereas the SED of ULASJ1234+0907 extends to longer wavelengths and only begins to drop off at $\sim 60\mu\text{m}$. This excess cool dust emission relative to pure AGN, could again be indicative of a starburst component. Further evidence for star formation is provided by the fact that the observed $500\mu\text{m}$ photometric data-point is not particularly well-fit by the models and lies above the model SEDs. At the redshift of this quasar, the [CII] cooling line is in the SPIRE $500\mu\text{m}$ band and can increase the broadband flux by 20-40% (Smail et al. 2011).

Our observations cannot directly rule out the presence of AGN heated cool dust distributed at larger radii from the central black-

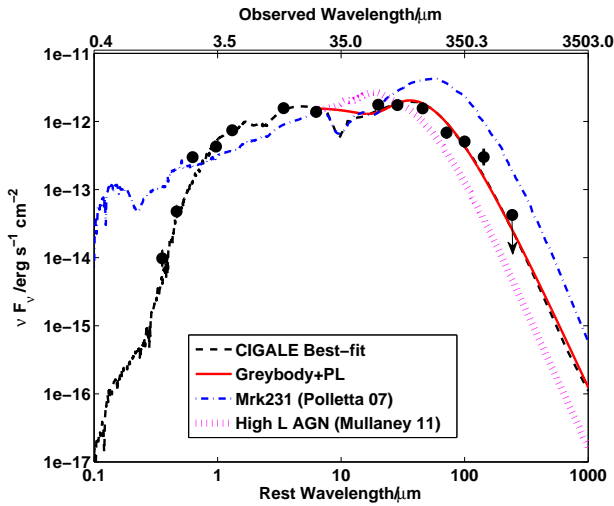


Figure 2. Best-fit SED to the observed photometry of ULASJ1234+0907 at $z = 2.503$ in units of νF_ν . The dashed line is the best-fit CIGALE SED which includes both AGN and starburst components while the solid line denotes the simple greybody plus mid-IR power-law fit to the data. We also show the SEDs of Mrk231 from Polletta et al. (2007) (dot-dashed line) and the high luminosity AGN from Mullaney et al. (2011) (dotted line). All SEDs have been scaled to match the rest-frame flux density of ULASJ1234+0907 at $\sim 6\mu\text{m}$ which corresponds to the observed-frame *WISE* $22\mu\text{m}$ band.

hole than the hotter dust responsible for the mid infrared emission. However, many FIR luminous quasars at high redshift have been demonstrated to contain significant reservoirs of molecular gas, which is unambiguous evidence for star formation (Wang et al. 2010). Furthermore, we demonstrate below using X-ray observations of the quasar, that the AGN bolometric luminosity inferred independently from the X-ray, is significantly lower than the total infra-red luminosity measured for this object. This once again hints that some additional source of heating apart from the AGN, may be responsible for the reprocessed far infra-red dust-emission. Regardless of the origin of the cool dust emission in the far infrared, we conclude that ULASJ1234+0907 is among the most far infrared luminous broad-line quasars known.

3.2 X-Ray Spectrum

In Figure 3, we plot the X-ray spectrum of ULASJ1234+0907 obtained using *XMM-Newton* together with the best-fit model spectrum fit using XSPEC. The model includes Galactic absorption plus intrinsic absorption (at $z = 2.5$) acting on a power law continuum with a narrow emission line at 6.4 keV to account for fluorescent Fe $K\alpha$. The total flux in the hard X-ray band covering 2 – 10 keV (observed frame) is $2.6 \times 10^{-14} \text{ erg s}^{-1} \text{ cm}^{-2}$ from the model fit. The (source rest-frame) hard X-ray luminosity is therefore $L_{2-10\text{keV}} = 1.3 \times 10^{45} \text{ erg/s}$ in our adopted cosmology. The best-fit photon index is 1.68 ± 0.25 and the inferred hydrogen column density is $N_H = (9.0 \pm 1.0) \times 10^{21} \text{ cm}^{-2}$. This column density agrees with the extinction of $A_V=6$ mags calculated from the near infrared broad-band colours in B12 assuming the dust properties are similar to our own Milky Way. The X-ray observations therefore indicate that ULASJ1234+0907 is also among the most X-ray luminous quasars known with a hard X-ray luminosity that

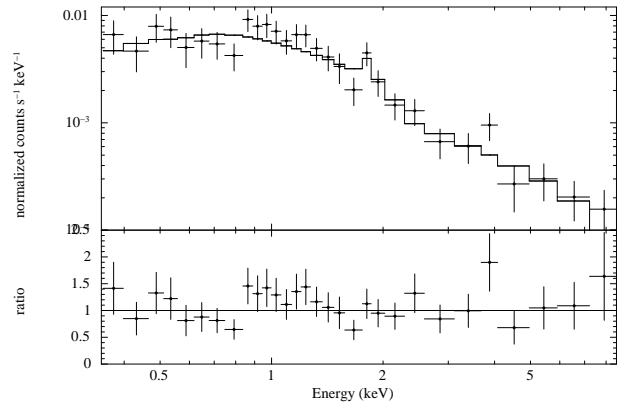


Figure 3. X-ray spectrum of ULASJ1234+0907 in the observed-frame together with the best-fit absorbed power-law model to this spectrum. The spectrum covers observed-frame energies of 0.4–8 keV corresponding to rest-frame energies of 1.4–28 keV.

is almost two orders of magnitude greater than Mrk231 and similar to the most powerful quasars in the Universe.

In the most powerful quasars accreting at close to the Eddington limit, the bolometric correction from the hard X-ray band is expected to be ~ 50 – 100 (Elvis et al. 1994). This implies that the AGN bolometric luminosity of ULASJ1234+0907 is $\sim 1.3 \times 10^{47} \text{ erg/s}$. Even assuming that all of this luminosity is seen as reprocessed dust emission in the far infrared, the shortfall in the total infrared luminosity calculated from the Herschel data, is still $\sim 1.7 \times 10^{47} \text{ erg/s}$. If this *missing* infrared luminosity is to come from star formation, we now obtain an even more extreme star formation rate in the quasar host galaxy of $\sim 6800 M_\odot/\text{yr}$. Conversely, we can consider the bolometric luminosity of ULASJ1234+0907 derived from the de-reddened UV luminosity: $L_{\text{bol}} = 1.9 \times 10^{48} \text{ erg/s}$ (B12). Based on this estimate of the bolometric luminosity and assuming a bolometric correction of ~ 100 , the X-ray luminosity is predicted to be $1.9 \times 10^{46} \text{ erg/s}$, more than an order of magnitude larger than what we measure. These discrepancies could indicate that the source is potentially X-ray weak.

The census of known AGN shows a remarkable lack of luminous, high Eddington ratio quasars that also have high columns of dust (Raimundo et al. 2010). These conditions are expected to drive strong outflows due to the effects of radiation pressure on the dust (Fabian 2012). The lack of very luminous, dusty quasars is perhaps not surprising given that most rapidly accreting quasars with high Eddington ratios have predominantly been selected at UV-optical wavelengths. In ULASJ1234+0907, the $A_V=6$ mags at $z = 2.5$ corresponds to 17.5 mags of extinction in the observed frame optical *i*-band. In other words, the quasar flux is suppressed by a factor of $\sim 10^7$ at optical wavelengths due to absorption by dust making it invisible in even the deepest optical surveys coming up within the next decade e.g. LSST.

Highly reddened Type 1 quasars like ULASJ1234+0907 that are accreting at close to the Eddington limit, are distinct from the well-studied obscured Type II AGN population. The FeK emission at rest-frame 6.4 keV (observed-frame 1.8 keV) in the quasar spectrum in Figure 3 is only marginally detected. The X-ray spectrum of ULASJ1234+0907 is therefore markedly different from typical Compton thick sources like NGC1068 where the FeK α line is much more prominent in the reflection dominated spectrum, and the photon index is considerably less steep. (Iwasawa et al. 1997).

3.3 Evidence against lensing

We have demonstrated that ULASJ1234+0907 is among the brightest and reddest broad-line quasars currently known with extremely high luminosities measured at both far infra-red and X-ray wavelengths. Given these extreme luminosities, we should consider the possibility of the quasar being lensed. The strongest evidence against lensing is provided by our deep i and K -band observations (Section 2). The optical image goes down to a magnitude limit of $i_{AB} < 25.15$. Even a high-redshift galaxy lens at $z > 1$ should have been easily visible at these depths. The quasar is undetected in the i -band and there are no other galaxies present within a $7''$ radius of the quasar position in this i -band image so there is no evidence to support the presence of a galaxy lens.

The K -band data from ISAAC was taken in $\sim 0.5''$ seeing which would allow us to easily resolve multiple emission sources associated with lensed images of the quasar, should they have been present. From Figure 1, we see that there is no evidence for multiple images in this sub-arcsecond seeing K -band data. The K -band emission from the quasar is unresolved and consistent with the size of the PSF. The lensing cross-section is therefore extremely small and the probability of lensing very low.

4 DISCUSSION & CONCLUSIONS

The above suite of multi-wavelength observations has allowed us to build up a comprehensive picture of the properties of ULASJ1234+0907, the reddest broad-line quasar currently known. With an X-ray luminosity of $L_{(2-10)keV} = 1.3 \times 10^{45}$ erg/s and a total infrared luminosity of $L_{TIR} = 3.1 \times 10^{47}$ erg/s, ULASJ1234+0907 is among the most luminous quasars known at both these wavelengths. Through sub-arcsecond, deep imaging of the quasar in the i and K -bands, we demonstrate that no galaxy lens is apparent in the optical and that the quasar emission is unresolved in the K -band. Lensing is therefore unlikely to be responsible for the extreme luminosities of this source. Even accounting for a large (62%) contribution of the AGN to the total infrared luminosity or assuming that only the FIR luminosity between 40 and $300\mu\text{m}$ is powered by a starburst, the estimated SFR in the host galaxy of this quasar is $> 2000 M_{\odot} \text{yr}^{-1}$. Measuring the AGN bolometric luminosity directly from the hard X-ray luminosity (assuming a bolometric correction of 100) and therefore requiring the rest of the total infra-red emission to be powered by a starburst, gives an even more extreme SFR of $\sim 6800 M_{\odot} \text{yr}^{-1}$. The column density inferred from the X-ray spectrum is $N_H = 9.0 \times 10^{21} \text{cm}^{-2}$ corresponding to $A_V = 6$.

Cosmological simulations, predict the existence of a high-Eddington ratio, luminous, reddened quasar phase which marks the transition of massive starburst galaxies to UV luminous quasars. This phase is distinct from the well-known Type II obscured AGN (Hopkins et al. 2008). During this phase, the bolometric output of both the starburst and AGN are expected to be at their peak. ULASJ1234+0907 has all the observed properties expected, were it to be detected during this transition phase - high luminosity and Eddington ratio, significant dust-reddening, broad emission lines and re-processed dust emission at far infra-red wavelengths. This quasar is an order of magnitude more luminous than the well-studied Submillimeter Galaxies (SMGs) and Dust Obscured Galaxies which have typically been selected over much smaller areas with *Spitzer* and/or SCUBA imaging. The black-hole mass is also considerably larger than measured in SMGs (B12). In terms of luminosity and space density, ULASJ1234+0907 is better matched

to the new population of HyLIRGs discovered using the *WISE*-All Sky Survey (Eisenhardt et al. 2012) although drawing evolutionary links between the *WISE* HyLIRGs and dust-reddened Type 1 quasars, would require detailed consideration of the relative lifetimes of these two phases, which is beyond the scope of this paper. We emphasise that reddened Type 1 quasars like ULASJ1234+0907 are distinct from the more highly obscured and less luminous Type II AGN where the dust extinction can often be explained by orientation effects. We have provided some evidence that the dust extinction in ULASJ1234+0907 arises on larger scales in the quasar host galaxy thus allowing the broad-line region to be viewed in the near infra-red. This dust is likely heated by both the AGN and a powerful starburst as would be expected during blowout. Although our observations do not directly detect AGN driven outflows, the combination of a supermassive black-hole accreting at close to the Eddington limit coupled with the high column density, is expected to drive strong outflows due to the effects of radiation pressure on dust.

The reddened quasar phase is unique in allowing us to study both the central accreting power-source (through X-ray and NIR spectroscopy) and the starburst host galaxy (through FIR photometry) in massive galaxies observed at the peak epoch of galaxy and black-hole formation. We are assembling multi-wavelength observations of much larger samples of these highly reddened Type 1 quasars which will inform theories of massive galaxy formation and be ideal testbeds for studying AGN feedback.

ACKNOWLEDGEMENTS

MB would like to thank Paul Hewett for many useful discussions. We thank Matt Auger for discussions on lensed quasars and Maud Galametz for help with the *Herschel* data reduction. Based on observations made with XMM-Newton, an ESA science mission with instruments and contributions directly funded by ESA Member States and NASA and the ESO Telescopes at the La Silla Paranal Observatory under programme ID: 290.A-5062.

REFERENCES

- Banerji M., McMahon R. G., Hewett P. C., Alaghband-Zadeh S., Gonzalez-Solares E., Venemans B. P., Hawthorn M. J., 2012, MNRAS, 427, 2275
- Banerji M., McMahon R. G., Hewett P. C., Gonzalez-Solares E., Koposov S. E., 2013, MNRAS, 429, L55
- Bendo G. J., et al., 2013, ArXiv e-prints
- Casey C. M., 2012, MNRAS, 425, 3094
- Coppin K. E. K., et al., 2008, MNRAS, 389, 45
- Croton D. J., et al., 2006, MNRAS, 365, 11
- Cutri R. M., et al., 2012, Technical report, Explanatory Supplement to the WISE All-Sky Data Release Products
- Dale D. A., Helou G., 2002, ApJ, 576, 159
- Davies J. I., et al., 2010, A&A, 518, L48
- Di Matteo T., Springel V., Hernquist L., 2005, Nature, 433, 604
- Eisenhardt P. R. M., et al., 2012, ApJ, 755, 173
- Elvis M., et al., 1994, ApJS, 95, 1
- Fabian A. C., 2012, ArA&A, 50, 455
- Fritz J., Franceschini A., Hatziminaoglou E., 2006, MNRAS, 366, 767
- González-Solares E. A., et al., 2011, MNRAS, 416, 927
- Gregg M. D., Lacy M., White R. L., Glikman E., Helfand D., Becker R. H., Brotherton M. S., 2002, ApJ, 564, 133
- Hewett P. C., Warren S. J., Leggett S. K., Hodgkin S. T., 2006, MNRAS, 367, 454

- Hickox R. C., et al., 2012, MNRAS, 421, 284
Hopkins P. F., Hernquist L., Cox T. J., Kereš D., 2008, ApJS, 175, 356
Iwasawa K., Fabian A. C., Matt G., 1997, MNRAS, 289, 443
Jansen F., et al., 2001, A&A, 365, L1
Kennicutt R. C., Evans N. J., 2012, ArA&A, 50, 531
Magorrian J., et al., 1998, AJ, 115, 2285
Mullaney J. R., Alexander D. M., Goulding A. D., Hickox R. C., 2011, MNRAS, 414, 1082
Noll S., Burgarella D., Giovannoli E., Buat V., Marcillac D., Muñoz-Mateos J. C., 2009, A&A, 507, 1793
Pilbratt G. L., et al., 2010, A&A, 518, L1
Poglitsch A., et al., 2010, A&A, 518, L2
Polletta M., et al., 2007, ApJ, 663, 81
Priddey R. S., Isaak K. G., McMahon R. G., Omont A., 2003, MNRAS, 339, 1183
Raimundo S. I., et al., 2010, MNRAS, 408, 1714
Roussel H., 2012, arXiv:1205.2576
Rowan-Robinson M., 2000, MNRAS, 316, 885
Smail I., Swinbank A. M., Ivison R. J., Ibar E., 2011, MNRAS, 414, L95
Wang R., et al., 2010, ApJ, 714, 699